Iron Oxide Nanoparticles as effective adsorbent and their application in removal Methyl red dye

Bahga Saleh[a], Samreen Fatema[a], Mazhar farooqui[a] and Shaikh Yusuf[b]

[a]Maulana Azad College of Arts, Science and Commerce, Aurangabad (MS), India.

[b]Shivaji College, Kannad (MS), India.

[b]Corresponding Author:shaikhyh@gmail.com

Abstract

The iron oxides nanoparticles have been synthesized by five different sol gel methods. Effect of calcination temperature on particle size, crystalline, morphology and chemical composition of the nanoparticles were studied with the assistance of particle size analysis, FT-IR Spectroscopy analysis, X-Ray Diffraction (XRD), Scanning Electron Microscopy (SEM) and energy dispersive x-ray (EDX). Out of these method five is additional appropriate and provides more correct and applicable results. The investigation process is carried out an adsorption study of all five NPs by different parameters such as effect of adsorbent dose, effect of concentration of dye, affect of pH, effect of contact time and effect of temperature were studied the adsorption capacity and adsorption behaviour of nanoparticals under various conditions. The experimental isotherm data has been studied. The kinetic study of the adsorption obeys Pseudo-first order and Pseudo-Second order models. The thermodynamic parameters namely Gibbs free energy, entropy, and enthalpy have revealed that the adsorption of methyl red on the nanoparticlas is s possible, spontaneous method and exothermic.

Keywords: Sol-gel, Nanoparticles, Methyl Red, FTIR, SEM-EDX, XRD.

FT-IR Spectroscopy, X-Ray Diffraction (XRD), Scanning Electron Microscopy (SEM) and energy dispersive x-ray (EDX).

Introduction

Nanosize materials have accepted important attention due to their outstanding physic-chemical properties. Nanoparticles are sub-micron moieties product of inorganic and organic materials that have several novel properties compared with bulk materials (diameter starting from 1-100 nm according to the used term,

although there is examples of nanoparticles many hundred of nanometer in size). The properties of nanoparticle can considerable altered by surface modification. [1]

Currently, there are two methods used to synthesize nanoparticles, referred because the top-down and bottom-up approaches. Briefly, within the top-down approach, nanoparticles are created by size reduction of bulk material by lithographic techniques and by mechanical techniques like machining and grinding , etc., while, in bottom-up method, tiny building blocks are assembled into a larger structure, e.g., chemical synthesis.[2]

Iron oxide is a transition metal which may exist in nature in several t forms. The most common are Magnetite (Fe_3O_4), Maghemite (γ-Fe_2O_3) and Hematite (α-Fe_2O_3). Maghemite and Magnetite, contain single domains with adiameter of around 5–20 nm. Magnetite is a common magnetic iron oxide that has inverse cubic inverse spinal structure with oxygen forming aclosed packing of 'fcc' and Fe cations occupying tetrahedral sites and octahedral sites shown in (Figure1). [3]

It is a black magnetic mineral and is ddditionally known as iron (II, III) oxide or ferrous ferrite. The chemical formula, Fe_3O_4, also can be written as $FeO.Fe_2O_3$ that consists of wüstite (FeO) and hematite (Fe_2O_3). Of all the natural minerals existing on the earth, it has the best magnetism. Maghemite may be a brown magnetic mineral that is found within the soils. It exhibits strong magnetism, and it is metastable with hematite and forms a continuous metastable solid solution with magnetite. α-Fe_2O_3 (hematite) exhibits weak ferromagnetism above about 260K T_M[4] ,in addition to the antiferromagnetism below 960 K. The Morin transition is called lowest. The observed weak ferromagnetism arises from the canting of the antiferromagnetically aligned spins above TM and this spin-canting angle is ≈5o. [5]

Iron oxides nanoparticles have a superb importance different field of science like chemistry, materials science and physics. It is one of the most foremost elementry nanoparticle having magnetic nature. Iron Oxide can be used for various applications like magnetic resonance imaging agent, sensing, cell labeling and sorting, as well as therapeutic applications like AC magnetic field-assisted cancer therapy, i.e. hyperthermia , giant Magnetoresistance for drug delivery , radionuclides , wastewater purification, such as to adsorb arsenate, chromium, cadmium, nickel. It can be used for alkalinity and hardness elimination, desalination, decolonization of tissue mill waste and removal of natural organic compounds. [6]

It is used for many technological applications in biology, such as extraction of genomic DNA, ultrahigh density magnetic storage media. For biological and biomedical applications, magnetic iron oxide nanoparticles are most popular material due of their biocompatibility, super paramagnetic behavior and chemical stability.

Nanoparticles have high magnetization values, a size smaller than 100 nm, and a narrow particle size distribution are required for all of these biomedical applications. Bioapplications supported magnetic nanoparticles (NPs) have gained vital attention as a result of NPs give specific benefits over different materials. For example, magnetic IONPs are cheap to produce, physically and with chemically stable, biocompatible, and environmentally safe. [8]

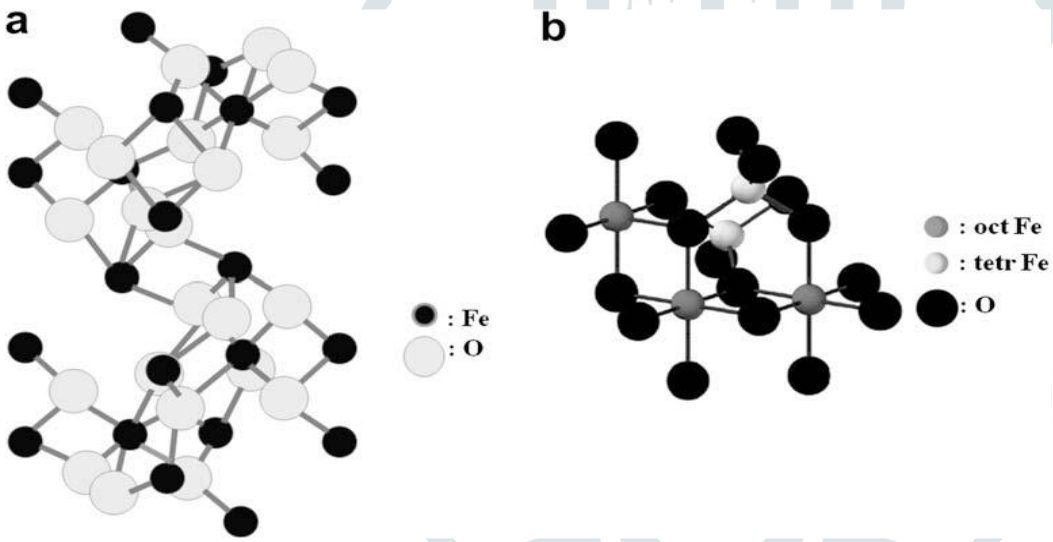

Figure1. Crystal structures of (a) hematite and (b) magnetite

Many advanced chemical processes, like the sol–gel process, electrostatic spray decomposition, hydrothermal, coprecipitation, water-in-oil emulsion method, electrostatic spray deposition, etc. are developed to prepare highly active materials of high purity and crystallinity.. [9]

Sol-gel method is widely used among processing routes, because of its significant advantages, like homogeneous mixing, sensible stoichiometric control, low synthesis temperature, short heating time, and uniform particle size, it is considered as the most effective one producing mesoporous structures and fine particles. [10]

Synthesis route is additionally vital to induce differing kinds of nanostructures with totally different properties. The control of the particle shape can be a major concern for nanostructured material synthesis as a result of electrical and optical properties of nanomaterials are sensitive on each size and shape of the particles. Therefore, it is desired to synthesize nano-material during a controllable shape and size by an easy approach. [11]

Dyes are often classified in many ways, according to chemical constitution, application category and finish use. Main dyes are grouped as acid dyes, basic dyes, direct dyes, mordant dyes, vat dyes, reactive dyes, disperse dyes, azodyes, and Sulphur dyes. [12]

The removal of dyes in an economic way remains a vital issue for researchers and environmentalists. [13] There are many strategies for removing dyes, which may be categorized into physical, chemical, and biological methods. Generally physical methods that adsorption, ion exchange, and membrane filtration are effective for removing reactive dyes while not manufacturing undesirable by-products. [14]

Recent researchers are focused on nanoparticles based adsorbents owing to its distinctive surface strucuture, composition and functionalism with compact size and less concentration adsorption. [15]

Nano-sized metal oxides have been shown to be effective materials as adsorbents because of their high surface reactivity, adsorption capacity and destructive sorbent compared to their industrial analogs, futher because the simple their synthesis from abundant natural minerals. [16]

The adsorption process has easy of design, a lot of economical, and simple to control, insensitive to toxic substances and cost effective. The effect of different variables such as contact time, pH, adsorbent dosage, effect of volume of dye solution. [17]

Methyl red MR is a standard dye that has three isomers (ortho-MR, meta-MR and Para-MR) with a -COOH group anchoring the benzene formula in varied positions. MR is often used as a dye pH scale indicator within the laboratory, ink-jet printing, textile industries and other commercial products. MR can cause disturbances within the eye, skin, and digestive tract if inhaled or ingested. [18]

In the present study, FeO nanoparticles have been synthesized by five different methods and characterized and used as adsorbent for adsorption study of Methyl Red (MR).

Materials and Methods

In this study, FeO is prepared by Sol-Gel method by five different ways. All five nanoparticles were characterized by FT-IR, SEM-EDX, XRD and subjected for adsoption on methyl red (MR) by different parameter i.e change in time, change in concentration of dye, change in weight of adsorbent, change in pH. The variation is reprsented by graph. For the present work double distilled water is used , iron chloride , sodium hydroxide ,potassium hydroxide, methanol , ethanol, oxalic acid , glacial acetic acid, and Methyl red (MR) were of AR grade from SD fine chemical Ltd India. The paid services of various labs were taken for FT-IR, SEM, EDX, XRD. Five methods were used for the preparartion of nanoparticles are as follow.

Method 1 (M1) 2gm of iron chloride was dissolved in 500 ml distilled water and kept on stirring. In another beaker HCl (36.5% HCl in distilled water) was prepared and 20 ml ethanol was added to iron solution and refluxed at 70 ^{0}C for 2 hrs, brown precipitate was appeared. The resulting gel was centrifuge for 10 min at 2000 rpm and washes several time with deionizer water. The residue mass dried in a hot air oven at 120^{o}c. The resulting compound underwent calcinations using muffle furnace at 450^0 C for two hrs to give iron oxide nanoparticles. [19]

Method 2 (M2) 2gm of iron chloride was dissolved in 200 ml of methanol and kept on stirring. In another beaker a solution of 6 gm of oxalic acid was dissolved in 200 ml of methanol and added to above warm solution to yield a thick gel and stirrer at 35 ^{o}C under constant stirring for 30 min. The resulting gel was centrifuge for 10 min at 2000 rpm and washes several times with deionizer water. The residue mass was dried in a hot air oven at 120^{o}c. The resulting compound underwent calcinations using muffle furnace at 450^0 C for two hrs to give iron oxide nanoparticles. [20]

Method 3 (M3) Synthesis of iron oxide nanoparticles by taking 9 gm of iron chloride and 5.4 gm of sodium hydroxide pellet were dissolved in 200 ml of methanol separately. The amount of methanol used was as minimum as required. Methanolic solution of iron chloride was kept on magnetic stirrer. Sodium hydroxide solution was added drop by drop with continuous stirring at room temperature for 3 hrs. The colour of the solution was turned to brown. The resulting gel was centrifuge for 10 min at 2000 rpm and washes several times with deionizer water. The residue mass dried in a hot air oven at 120 ^{o}c. The resulting compound underwent calcinations using muffle furnace at 450^0 C for two hrs to give iron oxide nanoparticles. [21]

Method4 (M4) 2gm iron chloride was dissolved in 500 ml distilled water. This solution was kept on stirring. To this stirr solution 1 ml of glacial acetic acid was added. The solution was heated at 100^{o}C for 30 min. Drop wise addition aqueous of sodium hydroxide 8M was carried out with continuous stirring. Till the colour of solution turned to brown. The resulting gel was centrifuge for 10 min at 2000 rpm and washes several time with deionisied water. The residue mass dried in a hot air oven at 120^{o}c. The resulting compound underwent calcination using muffle furnace at 450^{0} C for two hrs to give iron oxide nanoparticles. [22]

Method 5 (M5) Synthesis of iron oxide nanoparticles by taking 2 gm of iron chloride and 8M of KOH were dissolved in benzene and hexane mixture (1:1 ratio) separately. Solution of iron chloride was kept on magnetic stirrer. KOH solution was added drop by drop with continuous stirring. The solution was stirred and refluxed for 2 hrs. The resulting gel was centrifuge for 10 min at 2000 rpm and washes several times with deionizer water. The residue mass dried in a hot air oven at 120^{o}c. The resulting compound underwent calcinations using muffle furnace at 450^{0} C for two hrs to give iron oxide nanoparticles.[23]

The nanoparticles so formed were subjected to FT-IR, SEM, EDX and XRD analysis.

The adsorption study was carried out using batch adsorption method. The effect of initial concentration of dye, pH, adsorbent of dosage, contacts time etc was carried out as desorbed in earlier work. The nanoparticles were washed several times with distilled water till it becomes free from NaCl. Methyl red (MR) determined by using UV-visible spectrophotometer (S2-159) at λmax =420 nm. The adsorption experiment were carried out in stirred batch mode. For experiment, 10 ml of methyl red (MR) dye solution of specified concentration was continuously stirred unit 0.1 gm of powder at room temperature.

Result and Discussion

Fourier Transform Infrared Spectroscopy (FTIR) analysis

The structure and chemical compositions of iron oxide nanoparticles were examined in the 4000 – 400cm^{-1} region by using FT-IR spectroscopy analysis as shown in (Figure 2). FTIR exhibits various peaks at 420.406 cm^{-1}, 509.715cm^{-1} and 620.966 cm^{-1}574.683cm^{-1}, 632.537cm^{-1}, 991.232cm^{-1},1635.34 cm^{-1} and 3421.1 cm^{-1}. The peaks appeared at 420.406 cm^{-1}, 509.715cm^{-1}, 620.966 cm^{-1}, 574.683cm^{-1} and 632.537cm^{-1} are corresponding to iron–oxygen (FeO) and the peaks positioned at 1635.34 cm^{-1} and 3421.1 cm^{-1} are

corresponding to the bending vibration of absorbed water and surface hydroxyl and O H stretching mode. [24] [25]

The absorption bands at 528.4cm^{-1}, 586.254 cm^{-1} and 439.69 cm^{-1} which correspond to the Fe–O. [26]

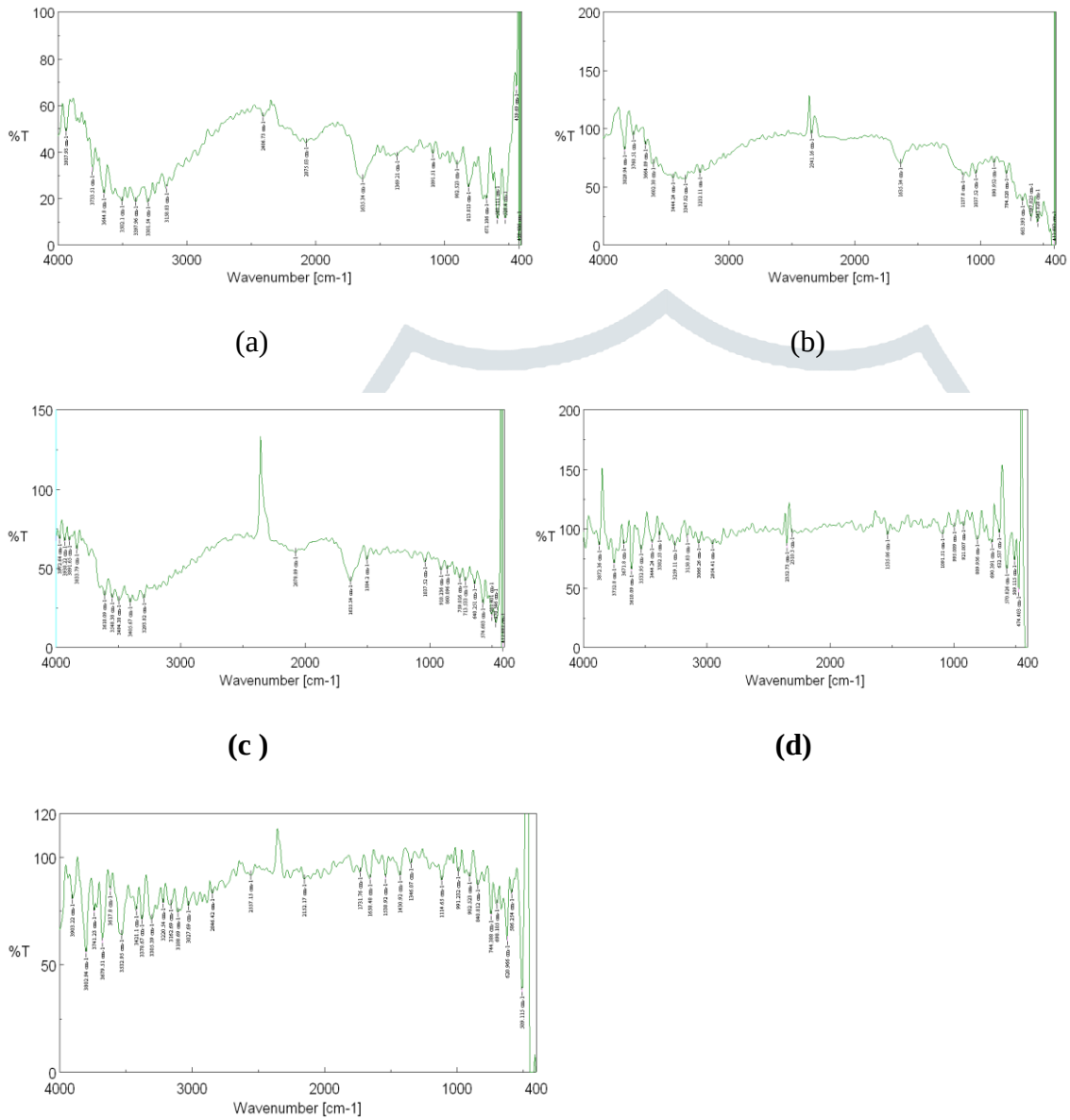

Figure2. FTIR of FeO Nanoparticles (a) Method 1 (b) Method 2 (c) Method 3 (d) Method 4 (e) Method 5.

Scanning Electron Microscopy and Energy dispersive X-ray (SEM-EDX)

Figure 3 shows SEM images illustrating the morphologies of FeO nanoparticles prepared with different methods via the sol gel method. As-prepared FeO nanoparticles by using $FeCl_2$. After calcinations at 450°C, product ($FeCl_2$) of tends to agglomerate with increasing the size. It can be seen from the image that the

particle size is in the range of nanometer having irregular morphology with different shapes and sized particles 16.7, 18.2, 21, 32.4, 29.6 (nm).

To check the chemical composition of synthesizes FeO nanoparticles was analysized by Energy dispersive X-ray .The spectrum shows the major peaks of Fe and O elements for FeO in nanoparticles and other peaks are also obtained in EDAX which may be due to the chemicals which were added during processing of nanoparticles were found in the EDAX spectrum as shown in (Figure 4)iron oxide nanoparticles synthesized by five procedures in which M5 gives more amounts of iron oxide nanoparticles is43.52 ± 0.14, while M1 gives least amount of nanoparticles that is 15.50 ± 0.15. Table1. Shows Percentage of all elements present in the nano powder.

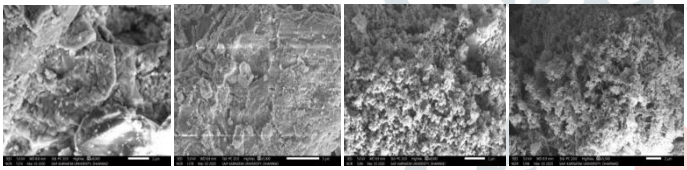

(a) **(b)**

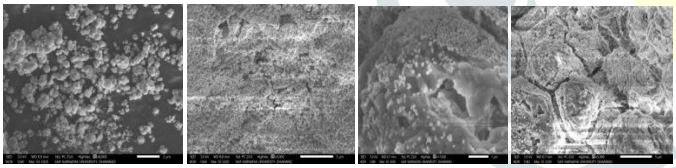

(c) **(d)**

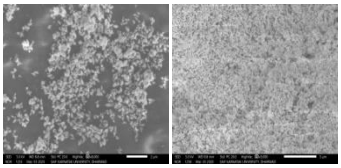

(e)

Figure3. SEM images of FeO Nanoparticles(a) Method 1 (b) Method 2 (c) Method 3 (d) Method 4 (e) Method 5.

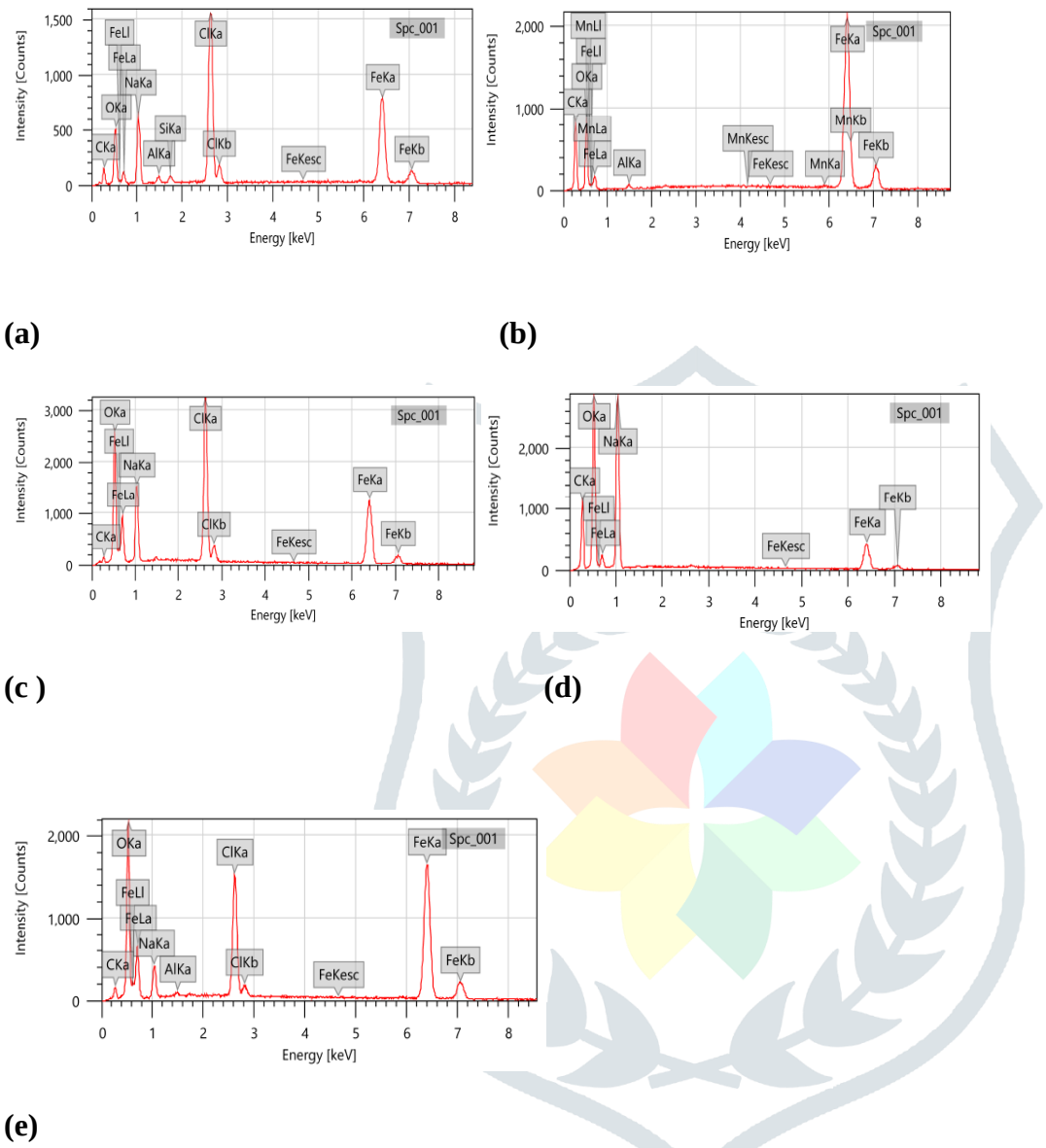

Figure4. EDAX of FeO Nanoparticles(a) Method 1 (b) Method 2 (c) Method 3 (d) Method 4 (e) Method 5

Table1. Percentage all elements present in the nano powder.

Element	M1	M2	M3	M4	M5
C	32.26± 0.49	50.36± 0.31	11.60± 0.21	35.65± 0.19	15.16 ± 0.23
O	26.76 ± 0.38	22.50± 0.26	50.39± 0.32	44.87± 0.26	50.42± 0.34
Na	12.39 ± 0.20	.....	9.60± 0.15	16.56± 0.12	6.22± 0.13
Cl	12.05 ± 0.10	.....	7.93± 0.07	.....	7.40 ± 0.06
Fe	15.50 ± 0.15	20.64± 0.16	41.49± 0.09	32.93± 0.04	43.52± 0.14

X-ray diffraction analysis (XRD)

X-ray Diffraction (XRD) is used to determine the crystal structure and phase. Figure5 illustrates XRD spectrum results of FeO nanopowder prepared by sol gel method.

M1 was recorded in the fraction angle range 5° to 40°. The diffraction peaks of iron oxide nanoparticles were observed at 2θ = 27.38º, 31.66º and 35. 62ºwhich can be indexed to (003), (111) and (201) planes of iron oxide nanoparticles respectively. The highest peak is at angle 31.66° at (111) plane with764.02 intensity.

M2 was recorded in the fraction angle range 5° to 20°. The diffraction peaks of iron oxide nanoparticles were observed at 2θ =5.95º, 6.79º, 7.85º, 9.46º, 10.45º, 11.64º, 12.46º, 13.72º, 14.38º, 15.04º, 17.09º, 18.24º and 19. 1º which can be indexed to (100), (101), (002), (110), (111), (200), (003), (103), (202), (210), (203), (104) and (302) planes of iron oxide nanoparticles respectively. The highest peak is at angle 10.45° at (111) plane with424.67 intensity.

M3 was recorded in the fraction angle range 5° to 50°. The diffraction peaks of iron oxide nanoparticles were observed at 2θ = 27.39º, 31.73º, 33.17º, 35.66º, and 45. 46ºwhich can be indexed to (220), (310), (311), (320) and (420) planes of iron oxide nanoparticles respectively. The highest peak is at angle 31.73° at (310) plane with 29617.54 intensity.

M4 was recorded in the fraction angle range 5° to 40°. The diffraction peaks of iron oxide nanoparticles were observed at 2θ =11.4º, 16.9º, 19.03º, 22.49º, 23.96.º, 25.03º, 26.84º, 28.13º, 29.68º, 32.54º, 33.63º, 35.5º and

36. 55ºwhich can be indexed to (110), (200), (211), (220), (221), (310), (311), (222), (320), (400), (322), (331) and (420) planes of iron oxide nanoparticles respectively. The highest peak is at angle 29.68ºat (320) plane with 33087.75intensity.

M5 was recorded in the fraction angle range 5° to 75°. The diffraction peaks of iron oxide nanoparticles were observed at 2θ =27.34º, 31.69º, 33.1º, 35.59º, 40.79.º, 45.4º, 49.39º, 53.97º, 56.45º, 62.36º, 63.93ºand 66. 2ºwhich can be indexed to (110), (200), (211), (220), (221), (310), (311), (222), (320), (400), (322), (331) and (420) planes of iron oxide nanoparticles respectively. The highest peak is at angle 31.69ºat (400) plane with 40939.48 intensity.

The average crystallite sizes (D) of samples were determined to be 45, 34.9, 46.3, 46.19, 43.49 and nm respectively according to the Debye- Scherrer equation.

$D=K\lambda/\beta\cos\theta$

Where

K: Constant = 0.9

λ is wave length of X-Ray (0.1541 nm).

β is FWHM (full width at half maximum) in radians.

θ is the diffraction angle .

D is crystalline diameter size.

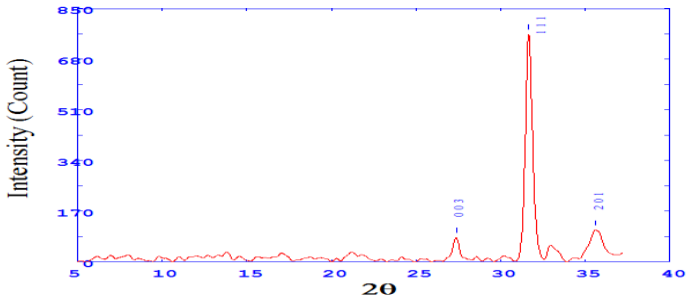
Intensity (Count)
2θ
003
111
201

(a)

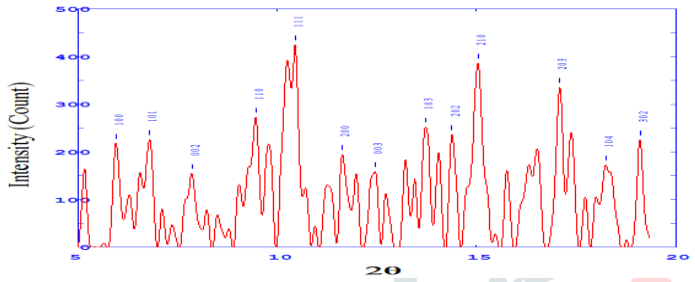
Intensity (Count)
2θ
100
101
002
110
111
200
003
103
202
210
203
104
302

(b)

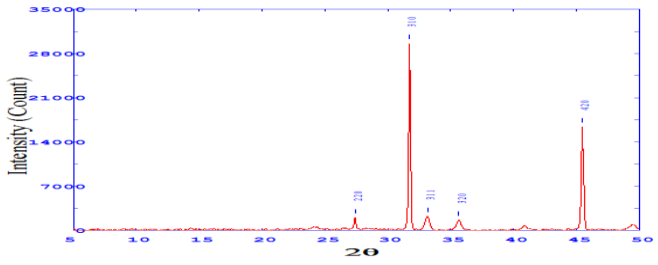
Intensity (Count)
2θ
220
310
311
320
420

(c)

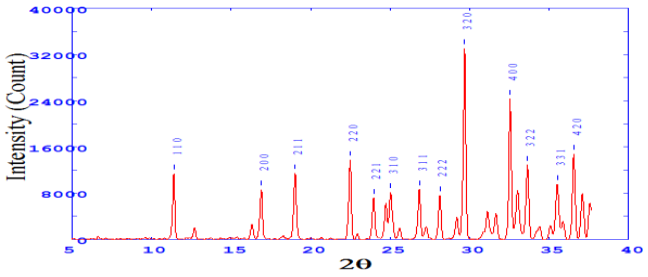

(d)

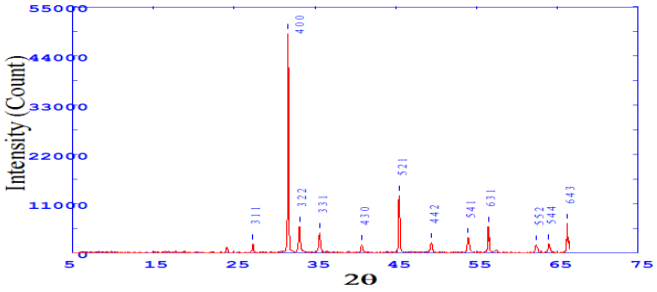

Figure5.XRD of FeO Nanoparticles (a) Method 1 (b) Method 2 (c) Method 3 (d) Method 4 (e) Method 5

Adsorption Study

Effect of contact time

In adsorption studies, effect of contact time plays important role regardless of different experimental parameters effecting adsorption kinetics. The sample of dye was taken in separate flasks and adsorption studies were carried out at various contact time from 5 – 25 min. The results are given in (Figure 6).

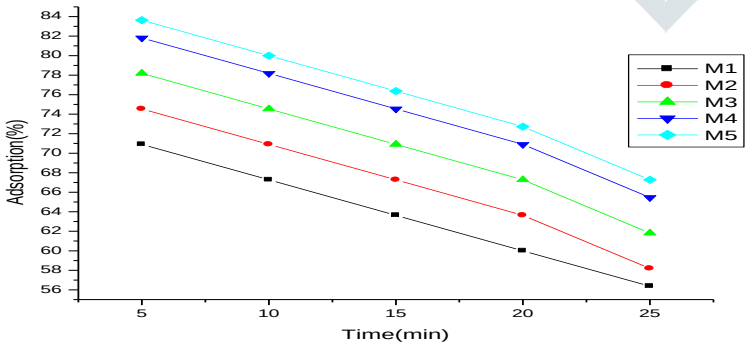

Figure 6. Effect of contact time

It is observed that adsorption decrease with increase in time, and the extent of adsorption varies with method of preparation but the nature of adsorption process seems to be same (Figure 6).

Effect of dosage

To examine the effect of the adsorbent dose on dye removal, 0.1 – 0.5 gm of adsorbent was added to 10 ml Methyl Red dye solution on five test tubes solution separately. The effect of adsorbent dosage on the percentage removal of MR dye is shown in (Figure7) adsorption increases with increase in dosage of adsorbent. It was observed that the removal efficiency was found at 0.5 gm adsorbent dose. i. e. the removal efficiency was higher at higher adsorbent dose.

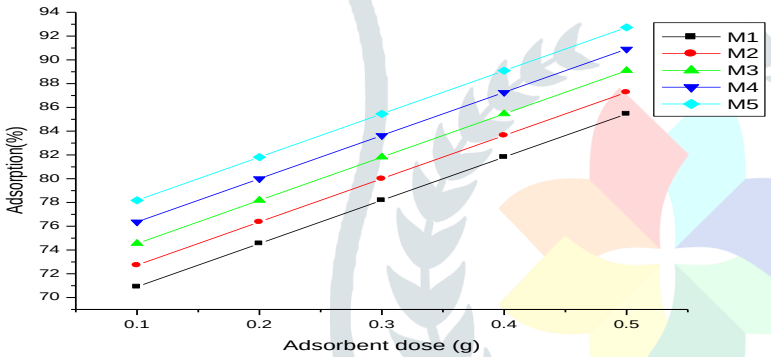

Figure7. Effect of adsorbent

Effect of initial concentration

The initial concentration of dye has a significant impact on its removal from aqueous solutions. The adsorption capacity decrease with increase initial concentration as shown in (Figure 8).

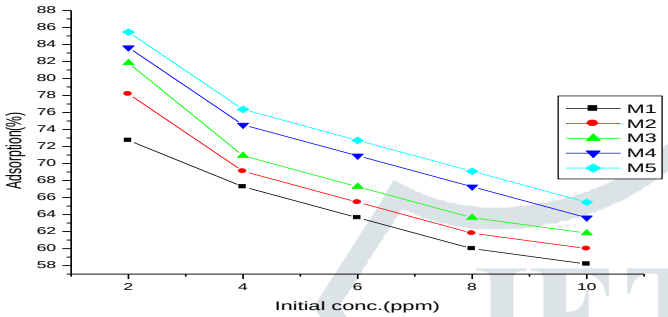

Figure8. Effect of initial concentration

Effect of pH

It is important to note that the solution pH imparts a significant role during the adsorption process. The effect of pH on MR dye removal is shown in (Figure 9). The maximum adsorption percentage occurred in both adsorbents at pH=2. I.e.acidic pH. The adsorption decreases till pH = 6. In basic pH adsorption get increases.

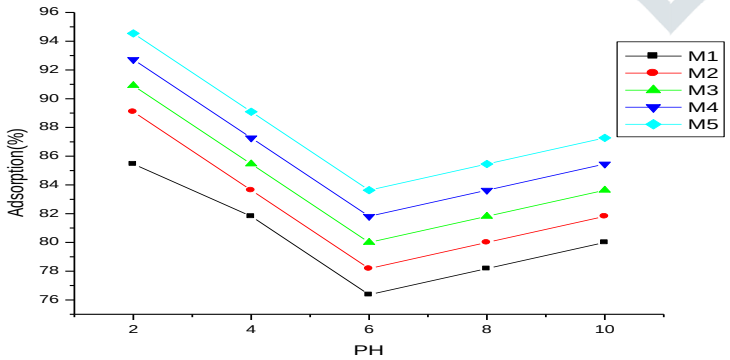

Figure 9. Effect of pH

Effect of temperature

Temperature is one of the most critical parameters affecting separation in most of the processes. The adsorption percentage of MR dye decreases with increase in temperature from 298 K to 318 K. from the graph it is observed that adsorption of dye on adsorbent is high at room temperature is shown in figure (10).

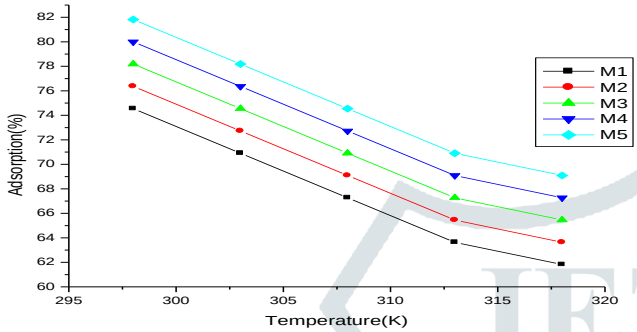

Figure10. Effect of temperature

Adsorption isotherm

In the present work, (table. 2) is shown Pseudo first order and Pseudo second order kinetic models forms as the following equations

$$Ln(Q_t - Q_e) = LnQ_e + K_1t \quad (1)$$

$$\frac{t}{Qt} = \frac{1}{K2Q2e} + \frac{t}{Qe} \quad (2)$$

Where Q_t (mg/gm) denotes the amount of adsorption at time t (min) , Q_e mg/gm) is the amount of adsorption at equilibrium are the amount of MR adsorbed at equilibrium and different time (min) and at equilibrium k_1 is the pseudo first order rate constant (min^{-1}). [27]

Table 2. kinetic parameter values of MR dye on FeO adsorbet

Method	Conc. Of MR (mg/L)	Pseudo-First order			Pseudo-Second order		
		K_1 (min^{-1})	**q_e (mg/gm)**	**R^2**	**K_2 (gm/mg.min)**	**q_e (mg/gm)**	**R^2**
M1	10	0.392899	762.9393	0.980496	-0.00011	5371.839	0.995405
M2	10	0.37222	902.298	0.99361	$-9.4x10^{-4}$	5565.45	0.992175
M3	10	0.476955	582.6396	0.986466	$-9.2x10^{-5}$	5924.346	0.992952
M4	10	0.46451	251.7561	0.993854	$-9.1x10^{-5}$	6282.709	0.99365
M5	10	0.91351	117.7742	0.981169	$-9x10^{-5}$	6462.913	0.993929

The presence of Langmuir adsorption monolayer on the outer surface of the adsorbent depends on the intermolecular potential between the adsorbent and the adsorbate.

Langmuir isotherm equation is:

$$\frac{C_e}{q_e} = [\frac{1}{Q_o}]\, C_e + \frac{1}{bQ_o} \quad (3)$$

Where C_e is the adsorbate equilibrium concentration (mg/L), q_e is the equilibrium concentration of dye on the adsorbent (mg/gm), Q_0 (mg/gm) b (L/mg) are Langmuir constants related to maximum monolayer adsorption capacity and energy of adsorption respectively. The values of Q_0 and b are calculated from the slope and intercept of plot $\frac{C_e}{q_e}$ against C_e. Langmuir isotherm can also be represented in terms of the separation factor (R_L), which is as follows:

$$R_L = \frac{1}{1+b\,C_o} \quad (4)$$

Where C_o is the initial concentration in (ppm), b is Langmuir constant. The values of R_L indicates the adsorption isotherm model of characteristic as follows R_L>1 (unfavorable), R_L=1 (Linear), 0 < R_L < 1 (favorable) and R_L= 0 (irreversible)

The Freundlich adsorption isotherm is used to explain the heterogeneity surface (1/n) of adsorbents. The linear form of the Freundlich equation is as follows:

$$\text{Log}Q_e = \text{Log}K_f + \frac{1}{n}\text{Log}\, C_e \quad (5)$$

C_e is the adsorbate equilibrium concentration (mg/L), Q_e is the amount of adsorbate equilibrium (mg/gm), K_f is Freundlich constant (mg/gm) (L/mg).[29]

Table .3 is shown Langmuir and Freundlich adsorption isotherm.

Table 3. Adsorption constant

Method	Conc. Of MR (mg/L)	Langmuir constant				Freundlich constant		
		Q_0 (mg/gm)	$b*10^{-5}$ (L/gm)	R_L	R^2	n	K_f (mg/gm.(L/gm))$^{1/n}$	R^2
M1	10	-214047	-0.02067	-0.93703	0.936366	0.510931	0.922401	0.880726
M2	10	-29082.1	-0.01719	-1.3903	0.927619	0.570064	1.701532	0.873141
M3	10	-46443.4	-0.01389	-2.5698	0.912235	0.63461	3.472962	0.865756
M4	10	-103145	-0.00836	6.089399	0.896601	0.717674	7.03218	0.856088
M5	10	520093.8	0.002307	0.812571	0.874169	0.829346	7.03218	0.842889

The effect of temperature in adsorption capacity is studied in between 25^0C and 45^0C. The various thermodynamic parameters are determined using equation:

$$\Delta G^o=\Delta H^o-T\Delta S^o \quad (6)$$

$$\text{Log}\left(\frac{qe}{ce}\right)=\frac{\Delta So}{2.303R}+\frac{-\Delta Ho}{2.303RT} \quad (7)$$

Were q_e is the amount of MR adsorbed per unit mass of NPs (mg / g) and c_e is the equilibrium concentration (mg / L).

The log (q_e / c_e) vs $\frac{1}{T}$ gives the values of ΔS^o and $-\Delta H^o$ as intercept and slope are shown in table.4.

Hence ΔG^o can be calculated is shown in table.5.

Table 4. values of enthalpy and entropy

Sr. No.	Method	ΔS^o	ΔH^o
1.	M1	5.177962	1593.55
2.	M2	-73.5392	24766.16
3.	M3	-75.9077	25722.99
4.	M4	-78.8117	26854.21
5.	M5	-82.3706	28198.32

Table 5. Thermodynamic parameter values

Sr. No.	Temp (K)	ΔG_0(M1)	ΔG_0(M2)	ΔG_0(M3)	ΔG_0(M4)	ΔG_0(M5)
1.	298	-2662.67	-2906.02	-3162.68	-3435.26	-3727.13
2.	303	-2244.89	-2471.29	-2707.34	-2954.78	-3215.74
3.	308	-1845.44	-2060.14	-2281.94	-2512.07	-2752.02
4.	313	-1456.54	-1663.37	-1875.4	-2093.58	-2318.98
5.	318	-1274.14	-1479.81	-1689.94	-1905.36	-2127.03

Conclusion

Iron oxide nanoparticles were synthesized using sol-gel method and its particle size, crystallite size, morphology and chemical composition were studied with varied characterization techniques. It may be noted that the size of synthesized iron oxide nanoparticles increase with calcination temperature due to agglomeration at elevated temperatures. All methods are good for the preparation of nanoparticals but five method is more appropriate and gives more amount of iron oxide nanopartical. The synthesized nanoparticals were studied for the removal of dyes from aqueous solution. The experimental isotherm data has been studied. The kinetic study of the adsorption obeys Pseudo-first order and Pseudo-Second order models. The

thermodynamic parameters namely Gibbs free energy, entropy, and enthalpy have revealed that the adsorption of methyl red on the nanoparticlas is s possible, spontaneous method and exothermic.

.

Acknowledgements

The authors thankfull to the karanataka university, Dharwad (KUD) for doing XRD and SEM in very affordable charge.

References

[1] Tharani, N. Synthesis and Characterization of Iron Oxide Nanoparticle by Precipitation.*Method In J of Adv R in PhySci (IJARPS).* 2015, 2(8),47-50.

[2] Sadia, A.; and Yongsheng,Green Synthesis of Iron Nanoparticles and TheirEnvironmental Applications and Implications. *J of Nanomaterials*. 2016, 6(209),3-26.

[3] Hasany, A.; Rajan , R. Systematic Review of the Preparation Techniques of Iron Oxide Magnetic Nanoparticles. *J of Nanosci and Nanotech*. 2012,2(6), 148-158.

[4]Hossein,Some Properties of Iron Oxide Nanoparticles Synthesized in Different Conditions. *World Appli Program(WAP j)*. 2013, 3(2),52-55.

[5]Tahir , A.; and Snobia, Synthesis of Iron Oxide, Cobalt oxide and Silver Nanoparticles by Different Techniques: A Review.*Int J of Sci& Eng R (IJSER)*. 2016,7(11),1178-1221 .

[6]Javier, L.; Giancarlo E de S.Synthesis and Characterization of Fe3O4 Nanoparticles with Perspectives in Biomedical Applications.*J of Materi R.* 2014, 17(3),542-549.

[7] Sara , Sh.; Shilpa, E. Preparation and characterization of magnetite nanoparticles by Sol-Gel method water treatment. *Int Journal of Inno R in Sci, Eng and Tech*.2013, 2(7), 2969-2973

[8]Mahnaz, M.; Haron, F.; Behzad, M.; and Jamileh, Synthesis, Surface Modification and Characterisation of Biocompatible Magnetic Iron Oxide Nanoparticles for Biomedical Applications. *J of Mol*. 2013,18, 7533-7548.

[9]Wei Wu, Z.Wu.; Taekyung, Ch.; andWoo-Sik. Recent progress on magnetic iron oxidenanoparticles: synthesis, surface functionalstrategies and biomedical applications. *J of Sci. Technol. Adv. Mater*. 2015,16,1-43.

[10]Ramdas, A.; Kulkarni, G.; Sivashanmugam, Preparation and electrochemical characterization of lithium cobalt oxide nanoparticles by modified sol–gel method. *J of MatRBull.* 2008, 43, 2497–2503.

[11]Gomaa, O.; and Salah, Electrical Properties of Cobalt Oxide/Silica Nanocomposites Obtained by Sol-Gel Technique.*Amer J of Eng and Appl Sci*. 2016,9(1), 12-16.

[12]Radwan,H.; and Chaieb,Adsorption of Crystal Violet Dye on Modified Bentonites.*Asian Jof Chem*.2016, 28(8), 1643-1647.

[13]Deepak , Sh.; ,Pardeep, Removal of methylene blue by adsorption onto activated carbon developed from Ficus carica bast.*Arabian J of Chem*.2017, 10, 1445–1451

[14] Subir , T.Adsorption of Reactive Blue 4 (RB4) onto Rice Husk in Aqueous Solution. *Int J of Sci& Eng R*. 2016,7(3), 7-12.

[15] Conrad, N.; Enenebeaku , I. Adsorption and Equilibrium Studies on the Removal of Methyl Red from Aqueous Solution Using White Potato Peel Powder.*Int J of Letters of Chem, Phy and Astro*. 2017,72, 52-64.

[16]Maryam, N.;Pari , B.;Reza &A. Adsorption of organic dyes using copper oxide nanoparticles: isotherm and kinetic studies.*J of Desalination and Water Treatment.* 2016, 57(52), 25278-25287.

[17]Ioannis , A.;Jie Fu, A.;&George,Use of nanoparticles for dye adsorption: Review. J*of Dispersion Sciand Tech*. 2018, 39(6), 3836-847.

[18]Parmvir , R'; Nirmal, K and Jayendra,Synthesis of manganese oxide NPs using similar process and different precursors-A comparative study.*Nanotech R J*. 2015, 8(3) ,419-427.

[19] Sanchez, l. (1995), Effect of the preparation method on the band gap of titania and platinum-titania sol-gel materials. *J of Mat latt*. 1995, 25, 271-275.

[20]Ismat, L.; Sarwaruddin, G.; Nuruzzaman, R. Preparation and Characterization of Copper Oxide NPs Synthesized via Chemical Precipitation Method.*Open Access Library J*. 2015, 2(3), 1-8.

[21] Hadeel, K.; Ahmed, Synthesis of copper oxide NPs via sol-gel method. (IJREI). 2017,1(4), 43-45.

[22] Rajesh, M.; Mazahar, Sh. Adsorption study for the Removal of Hazrdous Dye Congo Red by Biowaste Materials as Adsorbents. *(IJAIEM).*2016,5(11), 9-16.

[23]Hwang, A.; Dar, K.; and Badran,Synthesis and Characterization of Iron OxideNanoparticles for Phenyl Hydrazine Sensor Applications. *J of Sensor letters*. 2014,12,97-101.

[24] Seerangaraj, S.; Palanisamy, F.; Arivalagan, Biosynthesis of iron oxide nanoparticles using leaf extract of Ruellia tuberosa: Antimicrobial properties and their applications in photocatalytic degradation.*J of Photochemistry & Photobiology, B: Biology*. 2019,192, 74–82.

[25]Jiancheng, R.; Haiping, Z.; Xiaolong, Tao. Adsorption of methylene blue on modified electrolytic manganse residue: Kinetics, isotherm, thermodynamics and mechanism analysis.*J of Taiwan Inst of Chem Eng*.2018,82,351-359.

[26]Youssef, A.; Meryem, A.; Farid, Adsorption of methylene blue dye from aqueous solutions onto walnut shell powder: equilibrium and kinetics studies.*J of Surface and interfaces*. 2018, 11,74-81.

[27] Shidong , Ole.; Hon C L, N.; and Ludger , The Impact of Nanoparticle Adsorption on Transport and Wettability Alteration in Water-WetBerea Sandstone: An Experimental Study. *J of Frontiers in Physics*. 2019,7, 1-12.

[28]Nhamo , E.; Willis,Synthesis, characterisation and methyl orange adsorption capacity of ferric oxide–biochar nano-composites derived from pulp and paper sludge. *J of Appl Water Sci*.2017,7,2175–2186.

[29] Paul,Adsorption of methyi red and methyi orange using different three bark powder. *Acad R J*.2013,4(1), 330-338.